

This discussion paper is/has been under review for the journal Solid Earth (SE).
Please refer to the corresponding final paper in SE if available.

The Gregoriev Ice Cap length changes derived by 2-D ice flow line model for harmonic climate histories

Y. V. Konovalov and O. V. Nagornov

Department of Mathematics, National Research Nuclear University “MEPHI”,
Kashirskoe shosse, 31, 115409 Moscow, Russia

Received: 10 November 2009 – Accepted: 23 November 2009 – Published: 2 December 2009

Correspondence to: Y. V. Konovalov (yu-v-k@yandex.ru)

Published by Copernicus Publications on behalf of the European Geosciences Union.

Gregoriev Ice Cap length changes

Y. V. Konovalov and
O. V. Nagornov

Title Page

Abstract

Introduction

Conclusions

References

Tables

Figures

⏪

⏩

◀

▶

Back

Close

Full Screen / Esc

Printer-friendly Version

Interactive Discussion



Abstract

Different ice thickness distributions along the flow line and the flow line length changes of the Gregoriev Ice Cap, Terskey Ala-Tau, Central Asia, were obtained for some surface mass balance histories which can be considered as possible surface mass balances in the future. The ice cap modeling was performed by solving of steady state hydrodynamic equations in the case of low Reynolds number in the form of the mechanical equilibrium equation in terms of stress deviator components coupled with the continuity equation for incompressible fluid. The numerical solution was obtained by the finite difference method. A compound approximation of the ice surface boundary condition based on the extending of the mechanical equilibrium equation to ice surface points was applied. The approximation is considered as a way to overcome the problem of diagnostic equations numerical solution stability in the full model.

The basal sliding can arise in the glacier tongue at certain climatic conditions and was introduced both through linear and through non-linear friction laws.

A possible glacier length history, that corresponds to the regional climate changes derived from the tree-rings data, was obtained by the model.

The correlations between the glacier length changes and annual air temperature histories were investigated within the simplified equation introduced by J. Oerlemans in the form of linear dependence of annual air temperature versus glacier length and time derivative of the length. The parameters of the dependence were derived from modeled glacier length histories that correspond to harmonic climate histories. The parameters variations were investigated for different periodicities of harmonic climate histories and appropriate dependences are presented in the paper. The results of the modeling are in a good agreement with the J. Oerlemans climatic model.

SED

1, 55–91, 2009

Gregoriev Ice Cap length changes

Y. V. Konovalov and
O. V. Nagornov

Title Page

Abstract

Introduction

Conclusions

References

Tables

Figures

◀

▶

◀

▶

Back

Close

Full Screen / Esc

Printer-friendly Version

Interactive Discussion



1 Introduction

The Gregoriev Ice Cap (41°58' N, 77°55' E; Figs. 1 and 2) is the typical glacier of the plane-tops glaciers in the Central Asia. The plane-tops glaciers have average ice thicknesses in the range 100–150 m. The maxima of the glaciers lengths and of the glaciers widths are equal to 6 km and to 4 km respectively. The glaciers are located at the South slope of the Terskey Ala-Tau. They contain paleoenvironmental records in the Central Asia. Moreover they are sources of the fresh water in the region.

The objective of this study was the investigation of correlations between the modeled glacier length changes and the atmospheric temperature histories that were the model input data and were taken in the form of the harmonic temperatures. We sought the correlations in the form which is similar to the equation obtained early by J. Oerlemans based on calibrating a simple model of glacier dynamics with more explicit numerical modeling of a limited set of glaciers (Oerlemans, 2001, 2005).

The Ice Sheet Model Intercomparison Project for Higher-Order Models (ISMIP-HOM) (Pattyn et al., 2008) have revealed that modern higher-order (Hindmarsh, 2004) and full Stokes ice sheet models (Zwinger et al., 2007; Gagliardini and Zwinger, 2008) can be successfully applied in the cases of high basal topographic variability and slipperiness when the longitudinal stresses should be taken in to account. Hence, plane-tops glaciers modeling based on the higher-order and full Stokes ice sheet models can assign the glacier retreat/advance correctly and can give the qualitative forecasts of the glaciers evolution.

ISMIP-HOM results have shown that in general all participating models are in concordance. Full Stokes models closely agree with each other. Their spread of results is very low (<1%) and they give a results in concordance with analytical solutions based on the perturbation theory for a constant viscosity. In comparison to the full Stokes models the results of the higher-order approximations show larger spread (at the order of 2.5%). The higher spread is found for high aspect ratios where all stress components become important. Furthermore, the full Stokes models results anti-correlate with the ones of the higher-order models for the highest aspect ratio (0.2) (Pattyn et al., 2008).

SED

1, 55–91, 2009

Gregoriev Ice Cap length changes

Y. V. Konovalov and
O. V. Nagornov

Title Page

Abstract

Introduction

Conclusions

References

Tables

Figures

◀

▶

◀

▶

Back

Close

Full Screen / Esc

Printer-friendly Version

Interactive Discussion



Gregoriev Ice Cap length changes

Y. V. Konovalov and
O. V. Nagornov

Title Page

Abstract

Introduction

Conclusions

References

Tables

Figures

⏪

⏩

◀

▶

Back

Close

Full Screen / Esc

Printer-friendly Version

Interactive Discussion



The evolution of the Gregoriev Ice Cap in this paper was obtained by 2-D ice-sheet modeling and by using the ice surface mass balance measurements which were carried out in 1987 and 1988 (Fig. 3) (Mikhalenko, 1989). The developed 2-D ice sheet model is the 2-D steady state hydrodynamic model for incompressible fluid in the case of $Re \ll 1$, where Re is the Reynolds number, and the rheological Glen law. The model describes an ice flow along a flow line (Pattyn, 2000). It's supposed that the flow line is fixed in space (Figs. 1 and 2). The model contains a minimum of equations, the continuity equation for incompressible fluid and the mechanical equilibrium equation in terms of stress deviator components, and takes into account divergence/convergence of ice flow (Pattyn, 2000). The ice cap width increases from about 1.3 km at the summit to about 2.8 km at the front and we accounted the widening of the ice cap. The ice cap width changes with time were not accounted in the model. It seems the width variations with time can be properly obtained only by 3-D ice cap modeling taking into account the 3-D topographies of the ice cap surface and of the bed.

The compound approximation of the boundary conditions based on the extending of the mechanical equilibrium equation to ice surface points was applied to the stress-free ice surface. The approach is more effective for investigations of the problems such as a crevasses appearance due to seasonal changes of ice viscosity and stresses in a subsurface layer (Nagornov et al., 2006). The approach provides the numerical solution stability in the full 2-D flow line finite difference model developed in this paper in the case of ice and sea water interaction boundary.

2 Field equations

2.1 Diagnostic equations

Mathematical model for obtaining of the ice flow velocity in a steady-state glacier along a flow line includes the continuity equation for incompressible fluid, the mechanical equilibrium equation in terms of stress deviator components and the Glen law (Pattyn, 2000):

Gregoriev Ice Cap length changes

Y. V. Konovalov and
O. V. Nagornov

$$\begin{cases} \frac{\partial u}{\partial x} + \frac{u}{b} \frac{db}{dx} + \frac{\partial w}{\partial z} = 0; \\ 2 \frac{\partial \sigma'_{xx}}{\partial x} + \frac{\partial \sigma'_{yy}}{\partial x} + \frac{\partial^2}{\partial x^2} \int_z^{h_s} \sigma'_{xz} dz + \frac{\partial \sigma'_{xz}}{\partial z} = \rho g \frac{\partial h_s}{\partial x}; \\ \sigma'_{ik} = 2\eta \dot{\epsilon}_{ik}; \quad \eta = \frac{1}{2} [mA(T)]^{-\frac{1}{n}} \dot{\epsilon}^{\frac{1-n}{n}}; \\ 0 < x < L; \quad h_b(x) < z < h_s(x). \end{cases} \quad (1)$$

The description of the constants and variables in the equations of the paper are given in the Notation. The second equation of the system (1) stems from the mechanical equilibrium equations for a solid domain under the influence of the gravitation after the pressure exclusion. The manipulations lead to the two equations in the 3-D model or to the one equation in the 2-D flow line model, respectively, in terms of the stress deviator components.

Finally, taking into account the relations between deviatoric stresses and strain rates, the diagnostic equations can be written in the form of the system of two integro-differential equations for the flow velocity components (Pattyn, 2000, 2003):

$$\begin{cases} \frac{\partial u}{\partial x} + \frac{u}{b} \frac{db}{dx} + \frac{\partial w}{\partial z} = 0; \\ 4 \frac{\partial}{\partial x} \left(\eta \frac{\partial u}{\partial x} \right) + 2 \frac{\partial}{\partial x} \left(\eta \frac{u}{b} \frac{\partial b}{\partial x} \right) + \\ \frac{\partial^2}{\partial x^2} \int_z^{h_s} \eta \left(\frac{\partial u}{\partial z} + \frac{\partial w}{\partial x} \right) dz + \\ \frac{\partial}{\partial z} \left(\eta \frac{\partial u}{\partial z} \right) + \frac{\partial}{\partial z} \left(\eta \frac{\partial w}{\partial x} \right) = \rho g \frac{\partial h_s}{\partial x}. \end{cases} \quad (2)$$

The flow-law rate factor temperature dependence was taken from (Paterson, 1994).

[Title Page](#)
[Abstract](#)
[Introduction](#)
[Conclusions](#)
[References](#)
[Tables](#)
[Figures](#)
[Back](#)
[Close](#)
[Full Screen / Esc](#)
[Printer-friendly Version](#)
[Interactive Discussion](#)


2.2 Prognostic equation

The prediction of the ice thickness changes along the flow line as a response to time dependent environmental conditions is given by the mass balance equation or prognostic equation (MacAyeal et al., 1996):

$$5 \quad \frac{\partial H}{\partial t} = M_s - M_b - \frac{1}{b} \frac{\partial(\bar{u}Hb)}{\partial x} + \nu \frac{\partial^2 H}{\partial x^2}, \quad (3)$$

where \bar{u} is the depth averaged horizontal velocity.

The last term in the Eq. (3) provides the stability of the prognostic equation numerical solution. The instability can appear at high spatial resolution and in the case of steep velocity decrease, especially in glacier front vicinity, where ice thickness abruptly vanishes. The effect of the last term leads to the ice mass disappearance and depends on the artificial viscosity (ν). Hence, it's negative from the point of the mass conservation law, and it requires the choice of the artificial viscosity value as small as possible to achieve the numerical stability.

15 We considered non-zero artificial viscosity values close to the glacier front only, exactly, at the distance about 200 m upstream from the ice cap front point. The harmonic method of the numerical stability analysis leads to the expression for the non-zero viscosity values

$$20 \quad \nu_i = \nu_0 |u_i - u_{i-1}| \Delta x, \quad (4)$$

where Δx is the step of the grid, u_i is the horizontal velocity at the i -th grid node and the staggered grid convention is used (MacAyeal et al., 1996). In fact, the artificial viscosity depends on the velocity gradients at given spatial resolution and increases with the velocity gradients rise.

2.3 Heat transfer equation

25 The heat transfer in a glacier is a result of the thermal diffusion, horizontal and vertical advectons, and the deformational heating. Ice temperature changes along a flow line

Gregoriev Ice Cap length changes

Y. V. Konovalov and
O. V. Nagornov

Title Page

Abstract

Introduction

Conclusions

References

Tables

Figures

◀

▶

◀

▶

Back

Close

Full Screen / Esc

Printer-friendly Version

Interactive Discussion



are described by the heat transfer equation (Pattyn, 2000):

$$\frac{\partial T}{\partial t} = \chi \left(\frac{\partial^2 T}{\partial x^2} + \frac{1}{b} \frac{db}{dx} \frac{\partial T}{\partial x} + \frac{\partial^2 T}{\partial z^2} \right) - \left(u \frac{\partial T}{\partial x} + w \frac{\partial T}{\partial z} \right) + \frac{2A^{-\frac{1}{n}} \dot{\epsilon}^{\frac{1+n}{n}}}{\rho C}. \quad (5)$$

3 Boundary conditions

3.1 Boundary conditions at stress-free ice surface

It's supposed that the boundary conditions for the diagnostic Eq. (2) also should be written in the form of the two flow velocity equations. The first equation is the mass conservation equation per se. It's assumed that the incompressibility condition is valid at ice surface points.

The mechanical equilibrium equation can be extended to stress-free ice surface, but opposite to the continuity equation the mechanical equilibrium equation is not valid apart from the stress-free condition at ice surface points. Thus, the extension of the mechanical equilibrium equation to stress-free ice surface can be written as the system:

$$\begin{cases} \sigma'_{xz} = \alpha(2\sigma'_{xx} + \sigma'_{yy}); \alpha = \frac{\partial h_s}{\partial x} / \left[1 - \left(\frac{\partial h_s}{\partial x} \right)^2 \right]; \\ 2 \frac{\partial \sigma'_{xx}}{\partial x} + \frac{\partial \sigma'_{yy}}{\partial x} + \frac{\partial^2}{\partial x^2} \int_z^{h_s} \sigma'_{xz} dz + \frac{\partial \sigma'_{xz}}{\partial z} = \rho g \frac{\partial h_s}{\partial x}; \end{cases} \quad (6)$$

where first equation is the stress-free condition at ice surface in terms of stress deviator components.

The approach provides the solution stability in the full 2-D flow line finite difference model developed in this paper in the cases of different types of boundary conditions. Furthermore, the low spread of ISMIP-HOM results in the experiments A and E for the full Stokes models (Pattyn et al., 2008) proves that the approach provides second order (order of vanishing or smallness) of the boundary condition numerical approximation.

Title Page

Abstract

Introduction

Conclusions

References

Tables

Figures

◀

▶

◀

▶

Back

Close

Full Screen / Esc

Printer-friendly Version

Interactive Discussion



The surface temperature was applied as the boundary condition at the ice surface for the heat transfer Eq. (5). This temperature depends on the elevation (Makarevich et al., 1969) as

$$T_s(x, t) = T_{s0}(t) - 0.00233[h_s(x, t) - 4160] \quad (7)$$

where $T_{s0}(t)$ was taken as harmonic temperature in the non-steady experiments described below.

3.2 Basal boundary conditions

Borehole temperature measurements obtained in 2004 at the Gregoriev Ice Cap summit show that the ice temperature practically does not depend on vertical coordinate at the depths from 10 m to 45 m and is about -3°C (Arkhipov et al., 2004). It proves that, first, the ice is frozen to the bed ($v_b = 0$) and, second, the geothermal heat flux is close to zero, because non-zero geothermal heat fluxes provide noticeable temperature gradients in the steady-state profiles at these depths.

It is suggested, that the ice surface mass balance can increase significantly and steepen in time as a result of the climatic variability. Such climatic scenario leads to the ice flow increase. But no-slip basal boundary condition coupled with the incompressibility condition in the downstream hamper the upstream flow increase. Vice versa, the upstream flow forces the ice flow in the downstream but the ice flow velocity is relatively small due to no-slip basal boundary condition and is equal to zero at the lowest ice cap front point.

Thus, the contrariety can lead to instability of the numerical solution of the diagnostic Eq. (2). It should be underlined that the problem is not purely in the numerical solution but rather in the mathematical statement of the problem.

So, it is supposed that the basal sliding in the downstream can arise at some environmental changes. The slip boundary condition was applied only at the glacier tongue which was considered as the flow line subsection (Fig. 2) and was extended at about

Gregoriev Ice Cap length changes

Y. V. Konovalov and
O. V. Nagornov

Title Page

Abstract

Introduction

Conclusions

References

Tables

Figures

◀

▶

◀

▶

Back

Close

Full Screen / Esc

Printer-friendly Version

Interactive Discussion



600 m upstream along the flow line from the lowest front point. The friction law for the basal sliding in the case of small basal slopes is defined by equations

$$\begin{cases} (\sigma'_{xz})_b = \tilde{K}_{fr} |u_b|^{\frac{1-n}{n}} u_b; \\ w_b = 0; \end{cases} \quad (8)$$

and $\tilde{K}_{fr} = \begin{cases} K_{fr} & \text{if } n=1, \text{ linear friction law (MacAyeal, 1989, 1992);} \\ K_{fr} N^{\frac{1}{n}} & \text{if } n > 1, \text{ non-linear, Weertman-type friction law (Van der Veen, 1987);} \end{cases}$

5 where $N = \rho g H + (\sigma'_{zz})_b - \frac{\partial}{\partial x} \int_{h_b}^{h_s} \sigma'_{xz} dz$ - normal pressure at the base.

The common friction law, that takes into account bed slope variation, can be written as

$$\begin{cases} (2\sigma'_{xx} + \sigma'_{yy})_b \frac{dh_b}{dx} - (\sigma'_{xz})_b \left[1 - \left(\frac{dh_b}{dx} \right)^2 \right] = \\ = -\tilde{K}_{fr} \left(u_b + w_b \frac{dh_b}{dx} \right) \left| u_b + w_b \frac{dh_b}{dx} \right|^{\frac{1-n}{n}} \left(1 + \left(\frac{dh_b}{dx} \right)^2 \right)^{\frac{2n-1}{2n}}; \\ -u_b \frac{dh_b}{dx} + w_b = 0; \end{cases} \quad (9)$$

and, respectively, $N = \left(\rho g H + (\sigma'_{zz})_b - \frac{\partial}{\partial x} \int_{h_b}^{h_s} \sigma'_{xz} dz \right) / \sqrt{1 + \left(\frac{dh_b}{dx} \right)^2}$.

10 In this paper it's assumed that the no-slip/slip transition occurs gradually along the flow line. From the mathematical point it means that the friction coefficient along the flow line in the glacier tongue varies continuously from infinity to a constant value. So, the friction coefficient can be expressed in the form of the Laurent series

$$15 \quad K_{fr} = K_0 + \sum_{n=1}^{\infty} \frac{K_{-n}}{(x - X_{fr})^n}, \quad x > X_{fr}, \quad (10)$$

Gregoriev Ice Cap length changes

Y. V. Konovalov and
O. V. Nagornov

Title Page

Abstract

Introduction

Conclusions

References

Tables

Figures

◀

▶

◀

▶

Back

Close

Full Screen / Esc

Printer-friendly Version

Interactive Discussion



where X_{fr} is the boundary of the no-slip/slip transition. In essence, the friction coefficient changes along a flow line accordingly to the series (10) correspond to the ice thickness decrease. In practice, a few main terms of the series were considered.

The basal boundary condition for the heat transfer equation is assigned by the geothermal heat flux and the basal friction (Pattyn, 2000, 2003):

$$\frac{\partial T}{\partial z} = -\frac{1}{k} [Q + (\sigma'_{xz})_b u_b]. \quad (11)$$

3.3 Boundary conditions at the summit and at the front point

The boundary conditions at the summit ($x = 0$) are $u = 0$, $\sigma'_{xz} = 0$, $\partial h_s / \partial x = 0$.

The boundary conditions at the front point ($x = L$) are $u = 0$, $w = 0$ in the case of no-slip boundary condition over the whole flow line profile and the appropriate mass balance equation for the prognostic Eq. (3). In the case of the slip boundary condition we considered the linear interpolation of the depth averaged horizontal velocity from $(N - 2)$ -th and $(N - 1)$ -th nodes to the last N th node and the $w = 0$ approximation.

4 Numerical solution

The problem was solved by the finite difference method. The solution is based on the two-step algorithm (MacAyeal et al., 1996). First step involves solution of the non-linear diagnostic equations by an iterative procedure (Hindmarsh and Payne, 1996) for given flow line profile. The second step involves solutions of the heat transfer equation and of the prognostic equation to obtain ice temperature and ice thickness distributions along flow line, respectively, at next time step. To avoid the mass conservation problem the staggered-grid convention was used (MacAyeal et al., 1996).

To implement the finite differencing, arbitrary flow line profile is transformed into the rectangle by the coordinate transformation. The transformation is performed by replacing the vertical coordinate z with the dimensionless one: $\xi = (h_s - z)/H$ (Hindmarsh

Title Page

Abstract

Introduction

Conclusions

References

Tables

Figures

◀

▶

◀

▶

Back

Close

Full Screen / Esc

Printer-friendly Version

Interactive Discussion



and Hutter, 1988; Pattyn, 2000, 2003). The detailed description of the compound approximation of the boundary condition at stress-free ice surface, Eq. (6), is presented in Appendix A.

5 The ice cap evolution in the case of harmonic climate changes

The surface mass balance measurements were carried out at the Gregoriev Ice Cap flow line in 1987 and 1988 (Mikhalenko, 1989) (Fig. 3). The linear approximation of the averaged values for the two years is employed in this paper as the reference surface mass balance M_s .

The steady state experiments, when the model runs forward in time until a steady state for the reference surface mass balance is achieved, have shown, that the deviation between the modeled stationary glacier length and the observed length along the flow line is about 2% for the enhancement factor $m = 1$. Hence, there are no reasons to correct the flow-law rate factor values (Paterson, 1994) for the plane-tops glaciers. The modeled stationary ice surface for the reference surface mass balance and for $m = 1$ was taken as the initial ice surface in the non-steady experiments.

In the non-steady experiments the periodical climate variability was considered, when the annual air temperature varies as

$$T_a(t) = T_{a0} + \Delta T_a \sin \frac{2\pi t}{t_p}, \quad (12)$$

where t_p is the climate period, ΔT_a is the air temperature amplitude which was taken equal to 0.3°C and $T_{a0} = -3^\circ\text{C}$.

It was supposed that the annual air temperature and the ice surface mass balance vary proportionally and the dependence can be empirically expressed as

$$M_s(t) = M_{s0} - \Delta M_s \frac{T_a - T_{a0}}{\Delta T_a}, \quad (13)$$

Gregoriev Ice Cap length changes

Y. V. Konovalov and
O. V. Nagornov

Title Page

Abstract

Introduction

Conclusions

References

Tables

Figures

◀

▶

◀

▶

Back

Close

Full Screen / Esc

Printer-friendly Version

Interactive Discussion



where M_{s0} is the reference mass balance.

The mass balance and air temperature amplitudes relation is suggested unknown. The sign “-” before ΔM_s means that warming/cooling decreases/increases ice surface mass balance.

5 The experiments were carried out for different mass balance amplitudes ΔM_s in the range 0.2–0.6 m/a at the climate period $t_p = 500$ a (Fig. 4) and for different climate periodicity at the fixed amplitude $\Delta M_s = 0.4$ m/a (Fig. 5).

The basal sliding arises at certain time intervals when the ice mass grows. We considered the simple criteria of the no-slip/slip transition in the glacier tongue base with
10 time. It was formulated for the basal shear stress as $\max_{x_{tr} < x < L} (\sigma'_{xz})_b > \sigma_{cr}$, where σ_{cr} ,

the upper limit for the no-slip condition, was considered in the range $1\text{--}1.2 \times 10^5$ Pa. The ice flow velocity at $x = L$ changes abruptly at the points of the transitions and the derivative dL/dt has the break points, or points of discontinuity, at these moments. So, the curves $L(t)$ have the kinks or pikes at these points (Figs. 4 and 8). The no-
15 slip/slip transition at the beginning of the glacier advance occurs more smoothly in the case of non-linear friction law (Appendix B, Fig. B1). The friction coefficient values were considered as time-independent. More intensive ice mass growing requires more rapid glacier advance and, hence, smaller friction coefficient values. The values were chosen accordingly Eq. (10) and closely to a maximum as possible to avoid the
20 above mentioned instability (Sect. 3.2) in the diagnostic system solution. Thus, in the experiments the friction coefficient depends on the mass balance amplitude ΔM_s and decreases when the ΔM_s increases.

The glacier length oscillations periods are in concordance with the climate periods. Despite the nonlinearity of the diagnostic problem, the glacier length amplitude versus
25 the mass balance amplitude is close to the linear relationship (Fig. 6). While the deviation for $\Delta M_s = 0.6$ m/a can be explained by the bedrock topography inhibition (Fig. 7).

The tree-rings data collected at the Tien-Shan, ISTC, Project No. 2947, allowed to define the short-term climate periodicity in the region. The 12 a, 60 a and 110 a periodicity had been defined, and with assumption of existence of a long-term periodicity,

Gregoriev Ice Cap length changes

Y. V. Konovalov and
O. V. Nagornov

Title Page

Abstract

Introduction

Conclusions

References

Tables

Figures



Back

Close

Full Screen / Esc

Printer-friendly Version

Interactive Discussion



which was taken equal to 800 a, the superposition of the equal amplitudes $\Delta T_a = 0.2^\circ\text{C}$ and $\Delta M_s = 0.2\text{m/a}$ leads to the glacier length history, which is shown in Fig. 8. According to the glacier length amplitude versus mass balance periodicity (Fig. 5), short-term climate periodicity insignificantly affects the glacier length changes which are governed by the long-term component.

The melting rate at the base can be estimated as $M_b \approx (\sigma_{xz})_b u_b / \rho L_m \approx 0.01\text{m/a}$ for $(\sigma_{xz})_b \approx 10^5\text{ Pa}$ and $u_b \approx 10\text{ m/a}$ which were observed in the experiments. So the ice surface mass balance dominates in the prognostic equation.

The sensitivity of modeled glacier length history to different approximations of the friction law and to values of the artificial viscosity is represented in Appendix B.

6 The relationship between glacier length and annual air temperature

We investigated the correlations between the glacier length and the annual air temperature histories within the dependence, which was suggested by J. Oerlemans:

$$T_a(t) = \alpha + \beta L(t) + \gamma \frac{dL}{dt}. \quad (14)$$

The non-steady experiments prove that there are no unique parameters α , β and γ in Eq. (14), because the glacier length amplitude significantly depends on the climate periodicity at fixed air temperature amplitude and mass balance amplitude (Fig. 5). On the other hand, it seems that the main (long-term) climate period can be successfully derived from a glacier retreat/advance history based on the Eq. (14) and taking into account the dependences of α , β , γ versus the periodicity.

For given temperature history and glacier length changes obtained by ice flow modeling, the parameters α , β , γ satisfy the minimum of discrepancy between the left and the right sides of Eq. (14). The discrepancy minimum conditions lead to the linear

Gregoriev Ice Cap length changes

Y. V. Konovalov and
O. V. Nagornov

Title Page

Abstract

Introduction

Conclusions

References

Tables

Figures

◀

▶

◀

▶

Back

Close

Full Screen / Esc

Printer-friendly Version

Interactive Discussion



algebraic equations for α , β , γ obtaining:

$$\begin{cases} \alpha(t_2 - t_1) + \beta \int_{t_1}^{t_2} L dt + \gamma(L(t_2) - L(t_1)) = \int_{t_1}^{t_2} T_a dt; \\ \alpha \int_{t_1}^{t_2} L dt + \beta \int_{t_1}^{t_2} L^2 dt + \frac{\gamma}{2} (L^2(t_2) - L^2(t_1)) = \int_{t_1}^{t_2} T_a L dt; \\ \alpha(L(t_2) - L(t_1)) + \frac{\beta}{2} (L^2(t_2) - L^2(t_1)) + \gamma \int_{t_1}^{t_2} \left(\frac{dL}{dt}\right)^2 dt = T_a L \Big|_{t_1}^{t_2} + \int_{t_1}^{t_2} L \frac{dT_a}{dt} dt. \end{cases} \quad (15)$$

The major drawback of the air temperature reconstruction from the glacier length history according to Eq. (15) is the time derivative (dL/dt) sensitivity with respect to (i) bedrock undulation, (ii) features of glacier advance, with basal sliding or without it, (iii) front shape reorganization prior to retreat/advance beginning. We tried to overcome the problem by smoothing procedure which was applied to the glacier length history. At the first glance, the above mentioned features of the glacier flow are invisible in the glacier length history, but the success of the temperature reconstruction significantly depends on the “degree” of the glacier length history smoothing (Fig. 9).

On the other hand, the smoothing can deprive the possibility of the reconstruction of short-term temperature changes which weakly appear in the glacier history (Figs. 8 and 10). So, it’s difficult to point the optimal “degree” of glacier length history smoothing and the temperature paleoreconstruction requires coupling of independent methods such as moraine sediments analysis and, for example, the $\delta^{18}\text{O}$ data analysis or glacier surface temperature paleoreconstruction based on the borehole temperature measurements.

It seems, another way to overcome the problem is to introduce the initial phase φ_0 into the temperature-length relationship, i.e. to replace Eq. (14) with a new one in the form

$$T_a(\omega t + \varphi_0) = \alpha + \beta L(t). \quad (16)$$

Gregoriev Ice Cap length changes

Y. V. Konovalov and
O. V. Nagornov

Title Page

Abstract

Introduction

Conclusions

References

Tables

Figures



Back

Close

Full Screen / Esc

Printer-friendly Version

Interactive Discussion



The γ versus periodicity (Fig. 11) shows that the initial phase φ_0 sufficiently depends on the temperature harmonic oscillations frequency. The initial phase dispersion supposes that the reconstructed temperature can be a priori represented in the form of a part of the harmonic series. So, such approach application seems more poor beside the one based on the Eq. (14).

The frequency dependences (Fig. 11) are assigned by the lag between glacier length history and annual air temperature history (Fig. 4). The lag is formed as a result of the transition from the stationary condition to the non-stationary periodically condition. The maximum of the lag between steady-state glacier length history and mass balance history is achieved for high frequencies and is close to $t_p/2$ (or to π in radians) for $t_p = 100$ a. On the other hand, the initial phase φ_0 in Eq. (16) is close to zero because the mass balance history is in antiphase with respect to the annual air temperature history in the model. Thus, the parameter β is positive value and defines accordance between the terms of the left and the right sides of the Eq. (14) in the cases of high frequencies.

The lag between glacier length and mass balance histories decreases from about π to 0, when the frequency decreases from high values for about centennial climate changes to zero. Vice versa, the lag between glacier length and annual air temperature histories increases from 0 to π . In particular, φ_0 is about $\pi/2$ for $t_p \approx 550$ a, and the accordance between the left and the right sides of the Eq. (14) is defined mainly by the time derivative of the glacier length. Thus, the parameter β is approximately equal to zero at $\varphi_0 \approx \pi/2$ for similar and coherent glacier length and harmonic annual air temperature histories.

The parameters β and γ are in concordance with the values of the climate sensitivity and the response time, that were considered in the climatic model applied for the global temperature reconstruction in (Oerlemans, 2005), for $t_p \geq 800$ a (Fig. 11). If t_p is in the range 800–1200 a, then the climate sensitivity $c = -1/\beta$ varies in the range 8.2–11.7 km/K and the response time $\tau = \gamma/\beta$ varies in the range 227–320 a. The climate sensitivity and the response time in the Oerlemans climatic model (Oerlemans, 2005)

Gregoriev Ice Cap length changesY. V. Konovalov and
O. V. Nagornov

Title Page

Abstract

Introduction

Conclusions

References

Tables

Figures

◀

▶

◀

▶

Back

Close

Full Screen / Esc

Printer-friendly Version

Interactive Discussion



are expressed as

$$c = 2.3P^{0.6}s^{-1}, \quad \tau = 13.6\Delta^{-1}s^{-1}(1+20s)^{-0.5}L^{-0.5}, \quad (17)$$

where P is the annual precipitation in m/a, s is the mean surface slope of the glacier, Δ is the altitudinal mass balance gradient, and L is the reference glacier length. The estimation of the values for the Gregoriev Ice Cap by Eq. (17) gives $c \approx 10.1$ km/K and $\tau \approx 295$ a, where P was taken as average for the two years, 1987 and 1988, and is about 0.42 m/a (Mikhaleenko, 1989).

The recent warming and the Little Ice Age, which were reconstructed in (Oerlemans, 2005) by using of glacier length records, can be considered as parts of about millennial period, which contains the Medieval Warm Period, the Little Ice Age and the recent warming. Thus, the parameters β and γ can be treated accordingly to the Oerlemans climatic model but not for a wide spectrum of harmonic air temperature frequencies.

The parameters β and γ drop for $t_p = 600$ – 1200 a, if the mass balance amplitude decreases, and it is in accordance with the glacier length amplitude versus the mass balance amplitude (Fig. 6) and stems from Eq. (14). Accordingly Eq. (14), if L decreases p times, then the absolute values of β and γ increase p times for given temperature history. For example, for $t_p = 500$ a (Fig. 12) the term $|\gamma(dL/dt)|$ is higher than the term $|\beta L|$ at the order of the magnitude. Therefore, the $\gamma(dL/dt)$ defines the accordance between the left and the right sides of Eq. (14) for $t_p = 500$ a, and β is inessential. When the glacier length amplitude decreases approximately 1.42 times, the mass balance amplitude decreases from 0.5 m/a to 0.3 m/a (Fig. 6), the $|\gamma|$ rises 1.47 times and γ drops as negative value (Fig. 12). Therefore, the parameters β and γ are achieved the values in the corresponding ranges, 8.2–11.7 km/K for c and 227–320 a for τ , for smaller periods and for given air temperature amplitude if the mass balance amplitude decreases.

In other words, the values of β and γ decrease/increase for $t_p = 600$ – 1200 a depending on the ratio $\Delta M_s/\Delta T_a$ and in particular for $\Delta M_s/\Delta T_a \approx 1.3 \text{ m a}^{-1} \text{ K}^{-1}$ ($\Delta M_s = 0.4$ m/a, $\Delta T_a = 0.3^\circ\text{C}$) they are in a good agreement with the Oerlemans climatic model.

Gregoriev Ice Cap length changes

Y. V. Konovalov and
O. V. Nagornov

Title Page

Abstract

Introduction

Conclusions

References

Tables

Figures

◀

▶

◀

▶

Back

Close

Full Screen / Esc

Printer-friendly Version

Interactive Discussion



In a cases of harmonic air temperatures superposition the values of β and γ are defined by the main harmonica, and the reduction of the ratio $\Delta M_s / \Delta T_a$ to $1 \text{ m a}^{-1} \text{ K}^{-1}$ ($\Delta M_s = 0.2 \text{ m/a}$, $\Delta T_a = 0.2^\circ\text{C}$; Fig. 10) decreases the values to $\beta = -1.48 \times 10^{-4}$ ($c \approx 7 \text{ km/K}$) and to $\gamma = -3.23 \times 10^{-2} \text{ K a/m}$ ($\tau = 218 \text{ a}$).

The deviations in the curves in Fig. 11 as the result of the ratio $\Delta M_s / \Delta T_a$ variations can be estimated approximately by changing of ΔT_a in Eq. (12) and in Eq. (14). The boundaries of the deviations obtained for 50% variations of the ratio $\Delta M_s / \Delta T_a$ are represented in Fig. 11.

7 Conclusions

The results of the steady-state experiments show that deglaciation of the plane tops of Terskey Ala-Tau is observed for the significantly smaller values of the ice surface mass balance than the reference mass balance based on the experimental data which were obtained in 1987 and 1988. In particular, mass balance at the Gregoriev Ice Cap surface should be smaller by about 0.6 m/a than the reference one, and for the reference mass balance the glacier will be almost unchanged. Hence, the correct forecast of future glaciation/deglaciation of the plane tops requires the confirmation of the reference mass balance and resumption of monitoring of the ice surface mass balance changes.

The results of non-steady experiments show that, in general, annual air temperature history and glacier length history correlations for the harmonic climate changes are well described within the linear dependence of annual air temperature versus glacier length and time derivative of the length. In particular, the dependence is sensitive to the nature of the ice flow as well as to the bedrock undulations through the time derivative of the glacier length. Thus, the air temperature history reconstruction requires the smoothing of the glacier length history. On the other hand, the smoothing can lead to losses of data of short-term climate changes. The problems indicate that correct climate reconstruction requires integration of independent methods such as moraine

Gregoriev Ice Cap length changes

Y. V. Konovalov and
O. V. Nagornov

Title Page

Abstract

Introduction

Conclusions

References

Tables

Figures



Back

Close

Full Screen / Esc

Printer-friendly Version

Interactive Discussion



sediments analysis, $\delta^{18}\text{O}$ data analysis and glacier surface temperature paleoreconstruction based on the borehole temperature measurements.

5 The parameters β and γ of the temperature-length dependence are in a good agreement with the values of the climate sensitivity and the response time, respectively, in the Oerlemans climatic model for the periods of harmonic annual air temperature histories in the range 800–1200 a. These harmonic histories correspond to the period of the global temperature reconstruction implemented in (Oerlemans, 2005) because the recent warming and the Little Ice Age can be considered as parts of about millennial period, which contains the events like the Medieval Warm Period, the Little Ice Age and
10 the recent warming.

The ice flow modeling allows to obtain the parameters of the temperature-length dependence for different climate histories and the data can be collected for the future forecasts or climate reconstructions in the different regions of the Earth.

SED

1, 55–91, 2009

Gregoriev Ice Cap length changes

Y. V. Konovalov and
O. V. Nagornov

Title Page

Abstract

Introduction

Conclusions

References

Tables

Figures

⏪

⏩

◀

▶

Back

Close

Full Screen / Esc

Printer-friendly Version

Interactive Discussion



8 Notation

x	horizontal axis along a flow line, m.
z	vertical axis pointing upward ($z = 0$ at sea level), m.
t	temporary variable, a.
u	horizontal ice flow velocity, m a^{-1} .
w	vertical ice flow velocity, m a^{-1} .
L	length of a glacier flow line domain, m.
b	glacier width along a flow line, m.
H	ice thickness, m.
h_s	ice cap surface elevation, m.
h_b	bed elevation, m.
ρ	ice density, 900 kg m^{-3} .
g	gravitational acceleration, 9.8 m s^{-2} .
σ_{ik}	stress tensor components, Pa.
σ'_{ik}	stress deviator components, Pa.
$\dot{\epsilon}_{ik}$	strain-rate tensor components, a^{-1} .
$\dot{\epsilon}$	second strain-rate tensor invariant, a^{-1} .
η	ice effective viscosity, Pa a.
A	flow-law rate factor, $\text{Pa}^{-n} \text{ a}^{-1}$.
n	exponent in Glen's flow law, 3.
m	enhancement factor in the flow law.
T	ice temperature, K.
χ	ice thermal diffusivity, $35 \text{ m}^2 \text{ a}^{-1}$.
k	ice thermal conductivity, $2 \text{ W m}^{-1} \text{ K}^{-1}$.
C	ice heat capacity, $2 \times 10^3 \text{ J kg}^{-1} \text{ K}^{-1}$.
L_m	specific latent heat of ice fusion, $3.35 \times 10^5 \text{ J kg}^{-1}$.
M_s	mass balance at an ice surface, m a^{-1} .
M_b	melting rate at the base, m a^{-1} .
ν	artificial viscosity, $\text{m}^2 \text{ a}^{-1}$.
K_{fr}	friction coefficient, positive, Pa a m^{-1} .
Q	geothermal heat flux, W m^{-2} .

SED

1, 55–91, 2009

Gregoriev Ice Cap length changes

Y. V. Konovalov and
O. V. Nagornov

Title Page

Abstract

Introduction

Conclusions

References

Tables

Figures

◀

▶

◀

▶

Back

Close

Full Screen / Esc

Printer-friendly Version

Interactive Discussion



Approximation of the boundary condition at stress-free ice surface

The forms of the equations are modified after the coordinate transformation. In particular the second equation from the system (2) in variables x, ξ can be rewritten as

$$\begin{aligned}
 & 4 \frac{\partial}{\partial x} \left(\eta \frac{\partial u}{\partial x} \right) + 4 \frac{\partial}{\partial x} \left(\eta \xi'_x \frac{\partial u}{\partial \xi} \right) + 4 \xi'_x \frac{\partial}{\partial \xi} \left(\eta \frac{\partial u}{\partial x} \right) + 4 \xi'_x \frac{\partial}{\partial \xi} \left(\eta \xi'_x \frac{\partial u}{\partial \xi} \right) \\
 & + 2 \frac{\partial}{\partial x} \left(\eta \frac{u}{b} \frac{db}{dx} \right) + 2 \xi'_x \frac{\partial}{\partial \xi} \left(\eta \frac{u}{b} \frac{db}{dx} \right) \\
 & - 2 \xi'_x \frac{\partial}{\partial x} \left(\eta \frac{\partial u}{\partial \xi} \right) + 2 \xi'_x \frac{\partial}{\partial x} \left(H \eta \left(\frac{\partial w}{\partial x} + \xi'_x \frac{\partial w}{\partial \xi} \right) \right) \\
 & - \left(\xi''_{xx} - \frac{1}{H} H'_x \xi'_x \right) \eta \frac{\partial u}{\partial \xi} + \left(\xi''_{xx} - \frac{1}{H} H'_x \xi'_x \right) H \eta \left(\frac{\partial w}{\partial x} + \xi'_x \frac{\partial w}{\partial \xi} \right) \\
 & - \left(\xi'^2_x - \frac{1}{H^2} \right) \frac{\partial}{\partial \xi} \left(\eta \frac{\partial u}{\partial \xi} \right) + \left(\xi'^2_x - \frac{1}{H^2} \right) H \frac{\partial}{\partial \xi} \left(\eta \left(\frac{\partial w}{\partial x} + \xi'_x \frac{\partial w}{\partial \xi} \right) \right) \\
 & - \frac{\partial^2}{\partial x^2} \int_0^{\xi} \eta \frac{\partial u}{\partial \xi} d\tilde{\xi} + \frac{\partial^2}{\partial x^2} \int_0^{\xi} H \eta \left(\frac{\partial w}{\partial x} + \xi'_x \frac{\partial w}{\partial \xi} \right) d\tilde{\xi} = \rho g \frac{\partial h_s}{\partial x}
 \end{aligned} \tag{A1}$$

where $\xi'_x = \frac{1}{H} \frac{\partial h_s}{\partial x} - \frac{\xi}{H} \frac{\partial H}{\partial x}$ and $\xi''_{xx} = \frac{2}{H^2} \frac{\partial H}{\partial x} \left(\xi \frac{\partial H}{\partial x} - \frac{\partial h_s}{\partial x} \right) + \frac{1}{H} \left(\frac{\partial^2 h_s}{\partial x^2} - \xi \frac{\partial^2 H}{\partial x^2} \right)$.

The above mentioned alteration of Eq. (A1) to ice surface points requires to select the shear stress component σ'_{xz} and to replace it with $\alpha(2\sigma'_{xx} + \sigma'_{yy})$ in accordance with the stress-free surface condition in Eq. (6).

The terms of Eq. (A1) are grouped within certain order. The terms of the first and the second lines in Eq. (A1) represent the longitudinal stress gradients ($2 \frac{\partial \sigma'_{xx}}{\partial x}$ and $\frac{\partial \sigma'_{yy}}{\partial x}$) of the mechanical equilibrium equation from the system (1). They are unchangeable at ice surface points.

Gregoriev Ice Cap length changes

Y. V. Konovalov and
O. V. Nagornov

Title Page

Abstract

Introduction

Conclusions

References

Tables

Figures

◀

▶

◀

▶

Back

Close

Full Screen / Esc

Printer-friendly Version

Interactive Discussion



Gregoriev Ice Cap length changes

Y. V. Konovalov and
O. V. Nagornov

Title Page

Abstract

Introduction

Conclusions

References

Tables

Figures

◀

▶

◀

▶

Back

Close

Full Screen / Esc

Printer-friendly Version

Interactive Discussion



The third, fourth and fifth lines of Eq. (A1) are $2\xi'_x \frac{\partial}{\partial x} (H\sigma'_{xz})$, $(\xi''_{xx} - \frac{1}{H} H'_x \xi'_x) H\sigma'_{xz}$ and $(\xi'^2_x - \frac{1}{H^2}) \frac{\partial}{\partial \xi} (H\sigma'_{xz})$, respectively. These terms imply as the shear stress vertical gradient as the terms that arise due to the coordinate transformation and stem from the resistive stress gradient (Van der Veen and Whillans, 1989). They should be replaced in accordance with the stress-free condition in Eq. (6). It means that σ'_{xz} and $\frac{\partial}{\partial x} (H\sigma'_{xz})$ are equal to $\alpha(2\sigma'_{xx} + \sigma'_{yy})$ and to $\frac{\partial}{\partial x} (H\alpha(2\sigma'_{xx} + \sigma'_{yy}))$, respectively. But the $\frac{\partial}{\partial \xi} (H\sigma'_{xz})$ is equal to $\frac{1}{\Delta\xi} (H\sigma'_{xz})^2 - \frac{1}{\Delta\xi} H\alpha(2\sigma'_{xx} + \sigma'_{yy})^1$, where $\Delta\xi$ is the vertical grid size and upper index “1” means an ice surface grid point.

The integral terms of Eq. (A1) are equal to zero at ice surface points.

Appendix B

The deviations between glacier length histories obtained in a case of different model parameters

Since the sliding occurs only at the glacier tongue base, the glacier length deviations are inessential for considered friction law approximations by Eq. (8) and by Eq. (9), respectively (Fig. B1). The glacier length histories deviation was assessed for the linear friction law and it's insignificant, <1%.

The relative deviation for the linear and non-linear friction laws can be relatively small, is about 1%, due to the choice of the friction coefficient, that differs from the one in the linear friction law by multiplying of the series (10) at a constant value. Vice versa, if the friction coefficient in the non-linear friction law is known ($K_0 \approx 7 \times 10^2 \text{ Pa}^{\frac{n-1}{n}} \text{ a}^{\frac{1}{n}} \text{ m}^{-\frac{1}{n}}$ in Eq. (10)), then the deviation between the length histories can be insufficient in the case of relatively small area of sliding due to the choice of the friction coefficient in the linear approximation of the friction law.

For comparison, the deviation for the different vertical grid sizes, $N_\xi = 11$ and $N_\xi = 31$, achieves 2.5%. The effect of vertical resistive stress gradient, the integral term in Eq. (1) (Van der Veen and Whillans, 1989), accumulates in time, but also leads to insignificant length deviation, <2%, in the case of periodically climate changes. Thus, it is insignificant in the experiments.

Relatively small ν_0 in the artificial viscosity (4) also insufficiently distort glacier length history (Fig. B2). The deviation between the curves for $\nu_0 = 3$ and $\nu_0 = 5$ is about 1%.

Acknowledgements. The authors are grateful to the Ministry of Education and Science of Russia (Project No. P795).

References

- Arkipov, S. M., Mikhalenko, V. N., Kunakhovich, M. G., Dikikh, A. N., and Nagornov, O. V.: Thermal regime, ice types and accumulation in Grigoriev Glacier, Tien Shan, 1962–2001, *Data of Glaciological Studies*, 96, 77–83, 2004.
- Gagliardini, O. and Zwinger, T.: The ISMIP-HOM benchmark experiments performed using the Finite-Element code Elmer, *The Cryosphere*, 2, 67–76, 2008, <http://www.the-cryosphere-discuss.net/2/67/2008/>.
- Hindmarsh, R. C. A. and Hutter, K.: Numerical fixed domain mapping solution of free surface flows coupled with an evolving interior field, *Int. J. Numer. Anal. Methods Geomech.*, 12, 437–459, 1988.
- Hindmarsh, R. C. A. and Payne, A. J.: Time-step limits for stable solutions of the ice sheet equation, *Ann. Glaciol.*, 23, 74–85, 1996.
- Hindmarsh, R. C. A.: A Numerical Comparison of Approximations to the Stokes Equations used in Ice Sheet and Glacier Modeling, *J. Geophys. Res.*, 109, F01012, doi:10.1029/2003JF000065, 2004.
- MacAyeal, D. R.: Large-scale ice flow over a viscous basal sediment: Theory and application to ice stream B, Antarctica, *J. Geophys. Res.*, 94(B4), 4071–4088, 1989.
- MacAyeal, D. R.: The basal stress-distribution of Ice Stream-E, Antarctica, inferred by control methods, *J. Geophys. Res.-Solid Earth*, 97(B1), 595–603, 1992.
- MacAyeal, D., Rommelaere, V., Huybrechts, P., Hulbe, C., Determann, J., and Ritz, C.: An Ice-Shelf Model Test based on the Ross Ice Shelf, *Ann. Glaciol.*, 23, 46–51, 1996.

Gregoriev Ice Cap length changes

Y. V. Konovalov and
O. V. Nagornov

Title Page

Abstract

Introduction

Conclusions

References

Tables

Figures

◀

▶

◀

▶

Back

Close

Full Screen / Esc

Printer-friendly Version

Interactive Discussion



- Makarevich, K. G., Palgov, N. N., Tokmagambetov, G. A., Vilesov, E. N., Sudakov, P. A., Golovkova, B. G., Denisova, T. Ya., and Yegorova, N. D.: Glaciation of Zailiysky Alatau, Results of researches of International Geophysical Projects, IX section of IGY program, 23, 228 pp., 1969.
- 5 Mikhailenko, V. N.: Features of mass-exchange of plane-top glaciers of internal Tien-Shan, Data of Glaciological Studies, 65, 86–91, 1989.
- Nagornov, O., Konovalov, Yu., and Mikhailenko, V.: Prediction of thermodynamic state of the Gregoriev Ice Cap, Tien Shan, Central Asia, in the future, *Ann. Glaciol.*, 43, 307–312, 2006.
- 10 Pattyn, F.: Ice-sheet modeling at different spatial resolutions: focus on the grounding zone, *Ann. Glaciol.*, 31, 211–216, 2000.
- Pattyn, F.: A new three-dimensional higher-order thermomechanical ice sheet model: Basic sensitivity, ice stream development, and ice flow across subglacial lakes, *J. Geophys. Res.*, 108(B8), 2382, doi:10.1029/2002JB002329, 2003.
- 15 Pattyn, F., Perichon, L., Aschwanden, A., Breuer, B., de Smedt, B., Gagliardini, O., Gudmundsson, G. H., Hindmarsh, R. C. A., Hubbard, A., Johnson, J. V., Kleiner, T., Konovalov, Y., Martin, C., Payne, A. J., Pollard, D., Price, S., Rückamp, M., Saito, F., Soucek, O., Sugiyama, S., and Zwinger, T.: Benchmark experiments for higher-order and full-Stokes ice sheet models (ISMIPHOM), *The Cryosphere*, 2, 95–108, 2008, <http://www.the-cryosphere-discuss.net/2/95/2008/>.
- 20 Oerlemans, J.: *Glaciers and Climate Change*, A. A. Balkema Publishers, Rotterdam, Netherlands, 2001.
- Oerlemans, J.: Extracting a climate signal from 169 glacier records, *Science*, 308, 675–677, doi:10.1126/science.1107046, 2005.
- Van der Veen, C. J.: Longitudinal stresses and basal sliding: a comparative study, in: *Dynamics of the West Antarctic ice sheet*, edited by: Van der Veen, C. J. and Oerlemans, J., Dordrecht, etc., D. Reidel Publishing Co., 223–248, 1989.
- 25 Van der Veen, C. J. and Whillans, I. M.: Force Budget: I. Theory and Numerical Methods, *J. Glaciol.*, 35, 53–60, 1989.
- Vinogradov, O. N.: Surface ice flow velocities of the plane-top glaciers in the Tien-Shan, Data of Glaciological Studies, 6, 138–139, 1962.
- 30 Zwinger, T., Greve, R., Gagliardini, O., Shiraiwa, T., and Lyly, M.: A full Stokes-flow thermo-mechanical model for firn and ice applied to the Gorshkov crater glacier, Kamchatka, *Ann. Glaciol.*, 45, 29–37, 2007.

**Gregoriev Ice Cap
length changes**Y. V. Konovalov and
O. V. Nagornov

Title Page

Abstract

Introduction

Conclusions

References

Tables

Figures

◀

▶

◀

▶

Back

Close

Full Screen / Esc

Printer-friendly Version

Interactive Discussion



**Gregoriev Ice Cap
length changes**

Y. V. Konovalov and
O. V. Nagornov

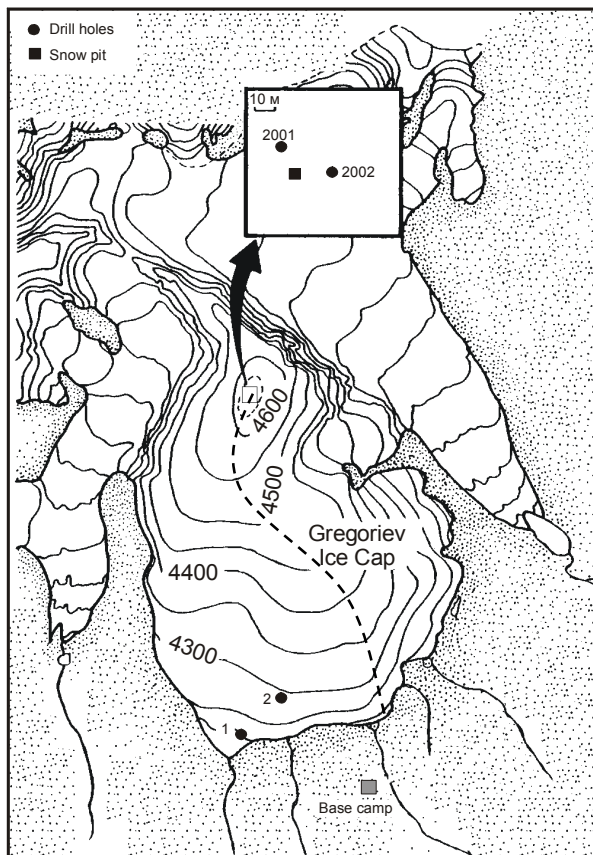


Fig. 1. The map of the Gregoriev Ice Cap. The dashed line represents the flow line.

Title Page

Abstract

Introduction

Conclusions

References

Tables

Figures

⏪

⏩

◀

▶

Back

Close

Full Screen / Esc

Printer-friendly Version

Interactive Discussion



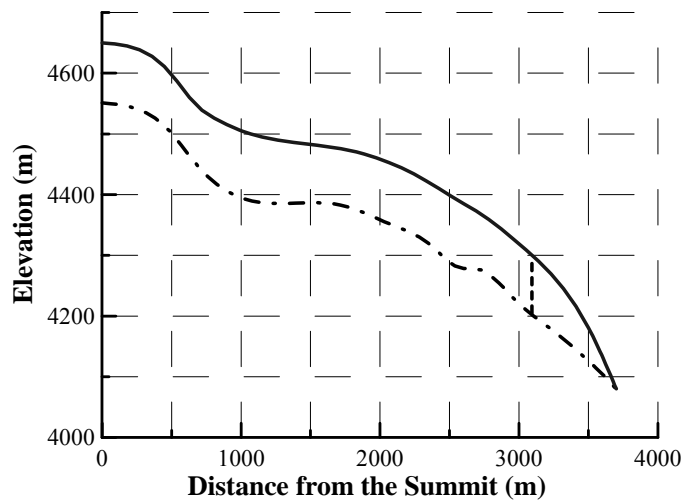
**Gregoriev Ice Cap
length changes**Y. V. Konovalov and
O. V. Nagornov

Fig. 2. The Gregoriev Ice Cap flow line profile. Vertical dashed line shows the no-slip/slip boundary in the model.

[Title Page](#)[Abstract](#)[Introduction](#)[Conclusions](#)[References](#)[Tables](#)[Figures](#)[◀](#)[▶](#)[◀](#)[▶](#)[Back](#)[Close](#)[Full Screen / Esc](#)[Printer-friendly Version](#)[Interactive Discussion](#)

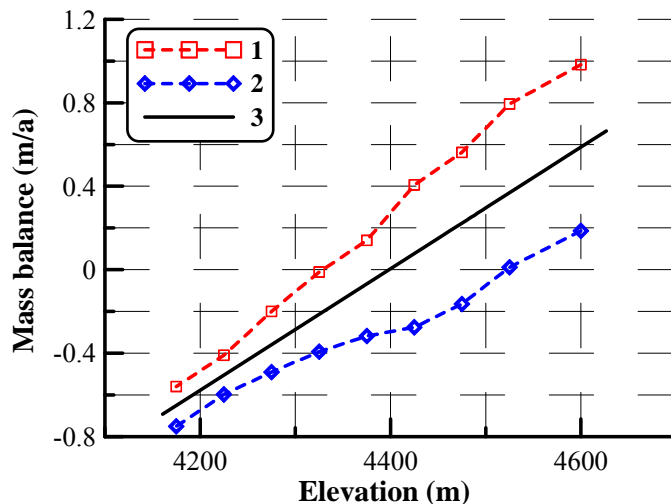
**Gregoriev Ice Cap
length changes**Y. V. Konovalov and
O. V. Nagornov

Fig. 3. Annual ice surface mass balance at the Gregoriev Ice Cap (Mikhalevko, 1989). 1 – experimental data, 1987; 2 – experimental data, 1988; 3 – linear approximation of the averaged data for the two years.

Title Page

Abstract

Introduction

Conclusions

References

Tables

Figures

◀

▶

◀

▶

Back

Close

Full Screen / Esc

Printer-friendly Version

Interactive Discussion



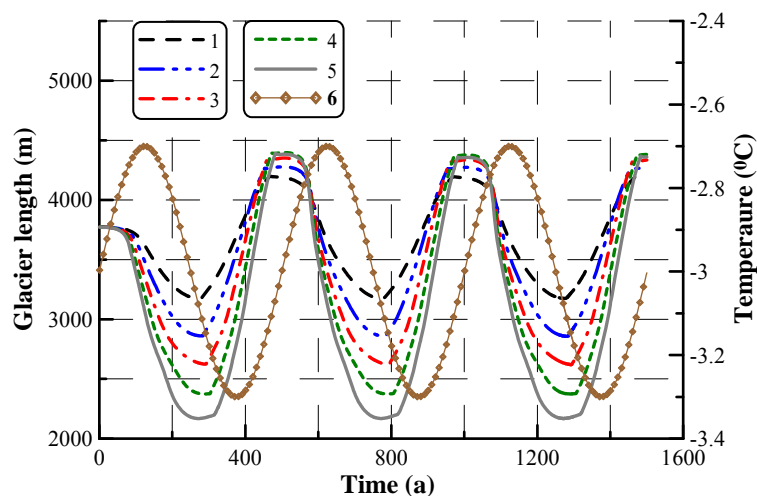
**Gregoriev Ice Cap
length changes**Y. V. Konovalov and
O. V. Nagornov

Fig. 4. The ice cap length changes in the non-steady experiments for harmonic ice surface mass balance changes with the amplitudes ΔM_s : **1** – 0.2 m/a; **2** – 0.3 m/a; **3** – 0.4 m/a; **4** – 0.5 m/a; **5** – 0.6 m/a. **6** – annual air temperature.

Title Page

Abstract

Introduction

Conclusions

References

Tables

Figures

◀

▶

◀

▶

Back

Close

Full Screen / Esc

Printer-friendly Version

Interactive Discussion



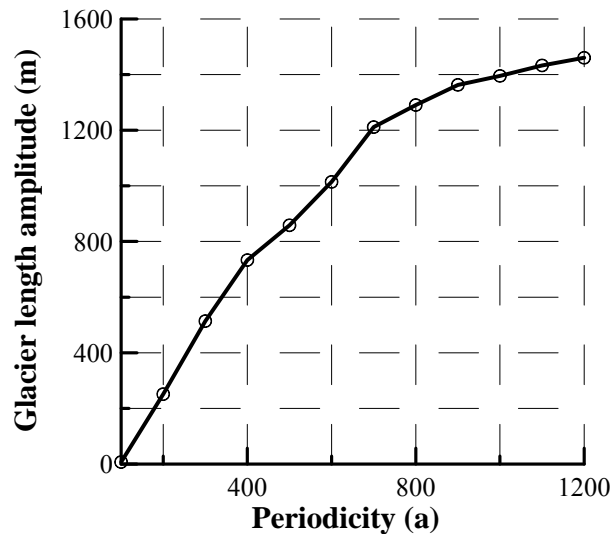
**Gregoriev Ice Cap
length changes**Y. V. Konovalov and
O. V. Nagornov

Fig. 5. The ice cap length oscillations amplitude versus climate periodicity in the case of harmonic climate variations, $\Delta M_s = 0.4$ m/a, $\Delta T_a = 0.3^\circ\text{C}$.

Title Page

Abstract

Introduction

Conclusions

References

Tables

Figures

◀

▶

◀

▶

Back

Close

Full Screen / Esc

Printer-friendly Version

Interactive Discussion



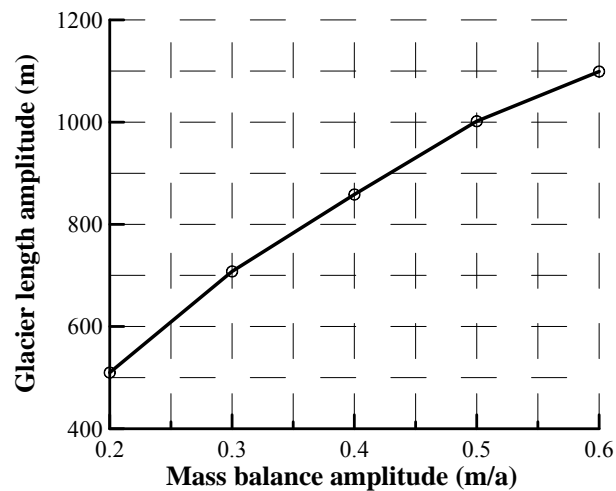
**Gregoriev Ice Cap
length changes**Y. V. Konovalov and
O. V. Nagornov

Fig. 6. The ice cap length oscillations amplitude versus surface mass balance amplitude in the case of harmonic climate variations, $t_p = 500$ a, $\Delta T_a = 0.3^\circ\text{C}$.

Title Page

Abstract

Introduction

Conclusions

References

Tables

Figures

◀

▶

◀

▶

Back

Close

Full Screen / Esc

Printer-friendly Version

Interactive Discussion



Gregoriev Ice Cap length changes

Y. V. Konovalov and
O. V. Nagornov

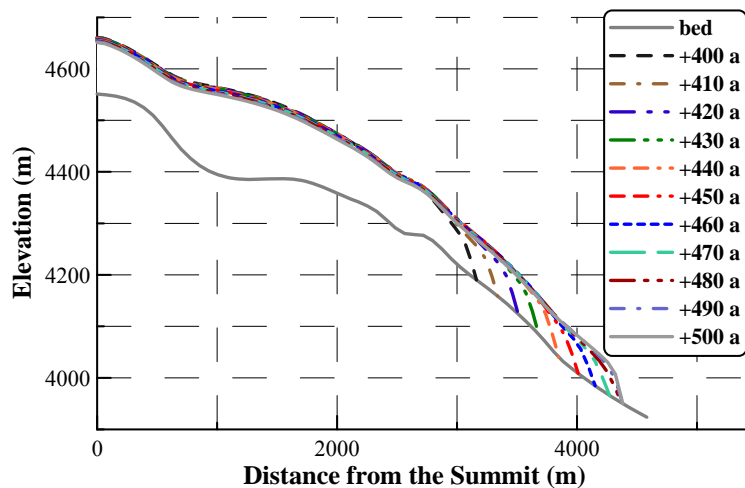


Fig. 7. The glacier advance in the case of the harmonic surface mass balance changes, $t_p = 500$ a, $\Delta M_s = 0.6$ m/a, $\Delta T_a = 0.3^\circ\text{C}$.

Title Page

Abstract

Introduction

Conclusions

References

Tables

Figures

◀

▶

◀

▶

Back

Close

Full Screen / Esc

Printer-friendly Version

Interactive Discussion



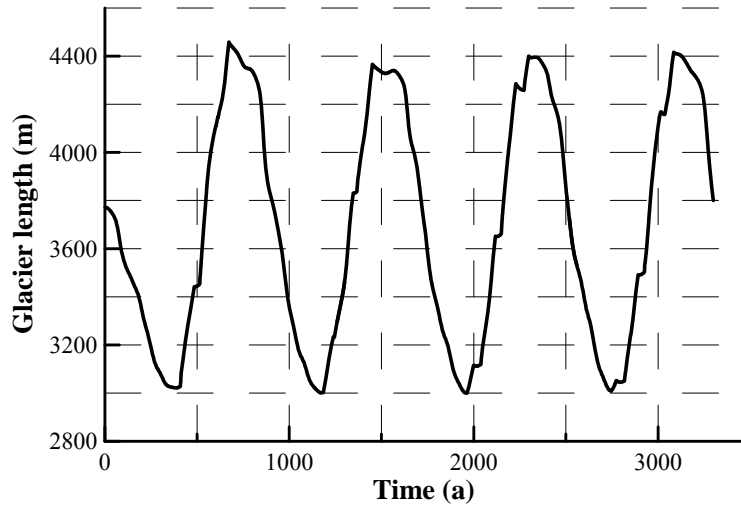
**Gregoriev Ice Cap
length changes**Y. V. Konovalov and
O. V. Nagornov

Fig. 8. The ice cap length history in the case of four harmonic surface mass balances superposition, $\Delta M_s = 0.2 \text{ m/a}$, $\Delta T_a = 0.2^\circ\text{C}$.

[Title Page](#)[Abstract](#)[Introduction](#)[Conclusions](#)[References](#)[Tables](#)[Figures](#)[◀](#)[▶](#)[◀](#)[▶](#)[Back](#)[Close](#)[Full Screen / Esc](#)[Printer-friendly Version](#)[Interactive Discussion](#)

Gregoriev Ice Cap length changes

Y. V. Konovalov and
O. V. Nagornov

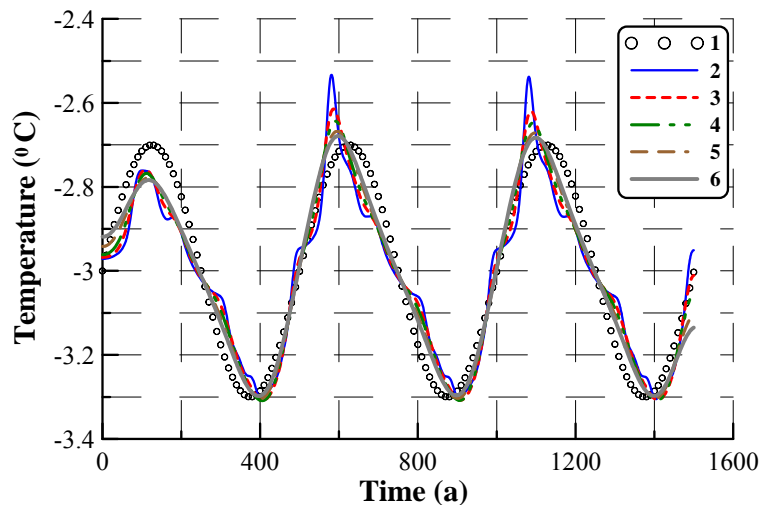


Fig. 9. The annual air temperatures derived from the ice cap length history for different “degrees” of smoothing of the ice cap length history. **1** – initial annual air temperature. The N_{sm} represents the number of the smoothing procedures which were applied to the ice cap length history: **2** – $N_{sm} = 10^2$; **3** – $N_{sm} = 5 \times 10^2$; **4** – $N_{sm} = 10^3$; **5** – $N_{sm} = 2 \times 10^3$; **6** – $N_{sm} = 3 \times 10^3$.

Title Page

Abstract

Introduction

Conclusions

References

Tables

Figures

◀

▶

◀

▶

Back

Close

Full Screen / Esc

Printer-friendly Version

Interactive Discussion



Gregoriev Ice Cap length changes

Y. V. Konovalov and
O. V. Nagornov

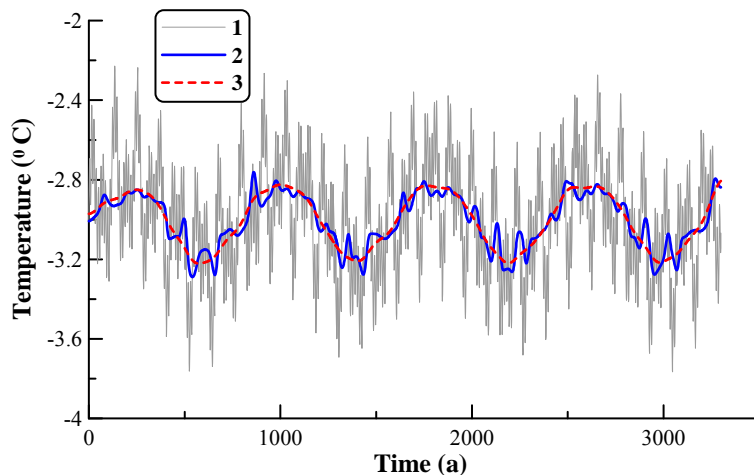


Fig. 10. The annual air temperatures derived from the ice cap length history in the case of four harmonic surface mass balances superposition, $\Delta M_s / \Delta T_a = 1 \text{ m a}^{-1} \text{ K}^{-1}$. **1** – initial annual air temperature. **2** – derived annual air temperature ($N_{sm} = 100$; $\beta = -1.28 \times 10^{-4} \text{ K/m}$; $\gamma = -2.78 \times 10^{-2} \text{ K a/m}$). **3** – derived annual air temperature ($N_{sm} = 3000$; $\beta = -1.48 \times 10^{-4} \text{ K/m}$; $\gamma = -3.23 \times 10^{-2} \text{ K a/m}$).

Title Page

Abstract

Introduction

Conclusions

References

Tables

Figures

◀

▶

◀

▶

Back

Close

Full Screen / Esc

Printer-friendly Version

Interactive Discussion



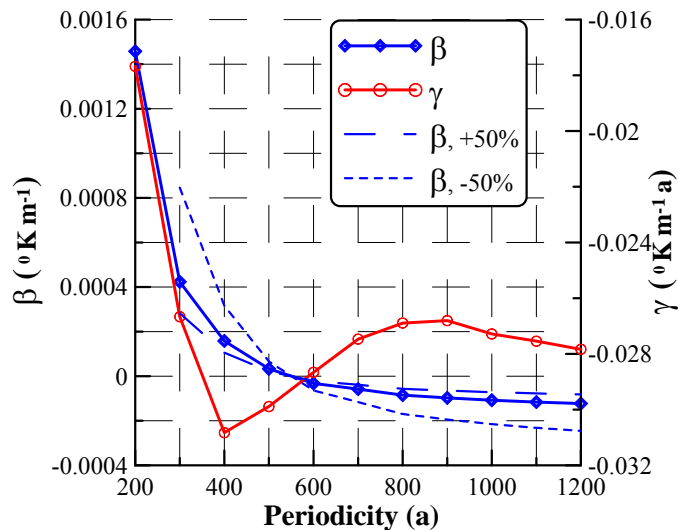
Gregoriev Ice Cap
length changesY. V. Konovalov and
O. V. Nagornov

Fig. 11. The results of β and γ calculations by Eq. (15) for different climate periodicity, $\Delta M_s = 0.4 \text{ m/a}$, $\Delta M_s/\Delta T_a \approx 1.3 \text{ m a}^{-1} \text{ K}^{-1}$. Dotted lines represent the boundaries of the deviations in β that correspond to 50% variations of the ratio $\Delta M_s/\Delta T_a$.

Title Page

Abstract

Introduction

Conclusions

References

Tables

Figures

◀

▶

◀

▶

Back

Close

Full Screen / Esc

Printer-friendly Version

Interactive Discussion



Gregoriev Ice Cap length changes

Y. V. Konovalov and
O. V. Nagornov

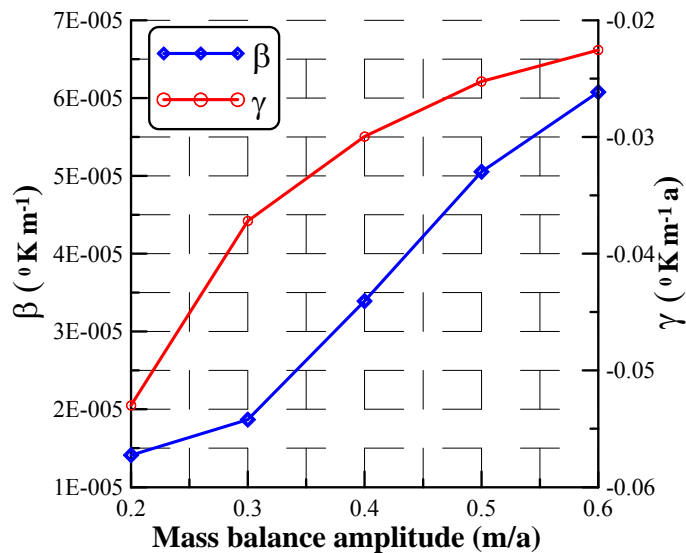


Fig. 12. The results of β and γ calculations by Eq. (15) for different mass balance amplitudes ($t_p = 500$ a).

[Title Page](#)
[Abstract](#)
[Introduction](#)
[Conclusions](#)
[References](#)
[Tables](#)
[Figures](#)
[◀](#)
[▶](#)
[◀](#)
[▶](#)
[Back](#)
[Close](#)
[Full Screen / Esc](#)
[Printer-friendly Version](#)
[Interactive Discussion](#)


Gregoriev Ice Cap length changes

Y. V. Konovalov and
O. V. Nagornov

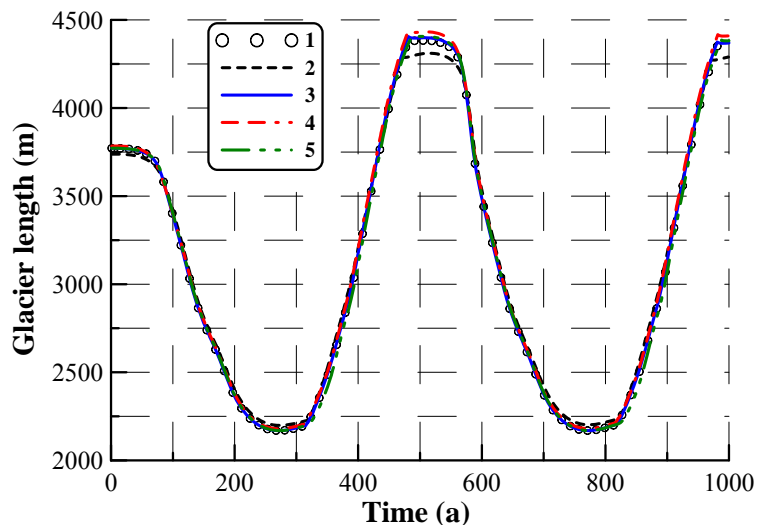


Fig. B1. The ice cap length history in the cases of different vertical grid sizes and different models: **1** – $N_{\xi} = 31$, basic model; **2** – $N_{\xi} = 11$, basic model; **3** – $N_{\xi} = 31$, the model with linear friction law in the form of Eq. (9); **4** – $N_{\xi} = 31$, the model without vertical resistive stress; **5** – $N_{\xi} = 31$, the model with non-linear friction law in the form of Eq. (9).

Title Page

Abstract

Introduction

Conclusions

References

Tables

Figures

◀

▶

◀

▶

Back

Close

Full Screen / Esc

Printer-friendly Version

Interactive Discussion



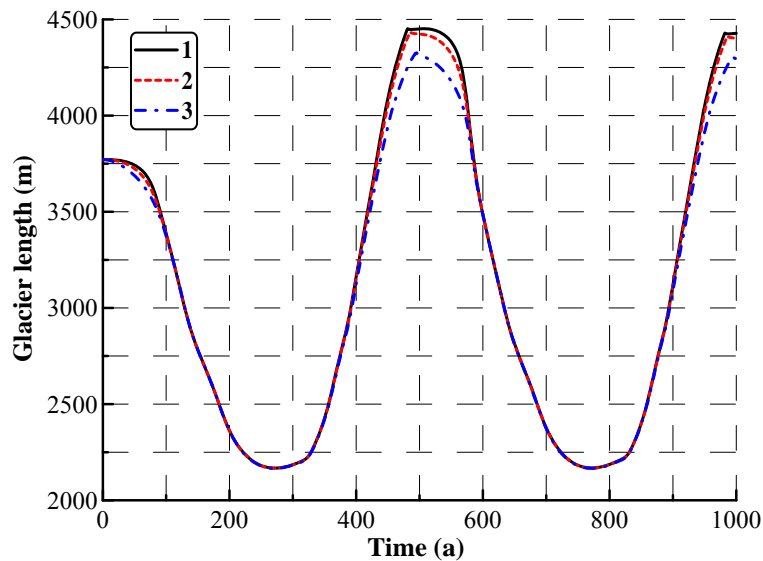
**Gregoriev Ice Cap
length changes**Y. V. Konovalov and
O. V. Nagornov

Fig. B2. The ice cap length histories obtained for different values of artificial viscosity: **1** – $\nu_0 = 3$; **2** – $\nu_0 = 5$; **3** – $\nu_0 = 10$.

Title Page

Abstract

Introduction

Conclusions

References

Tables

Figures

◀

▶

◀

▶

Back

Close

Full Screen / Esc

Printer-friendly Version

Interactive Discussion

